Electron spin echo detection of the microwave-induced recombination of transient radical pairs produced in photochemical reactions

ARTICLE *in* THE JOURNAL OF CHEMICAL PHYSICS · JUNE 1997

Impact Factor: 2.95 · DOI: 10.1063/1.474022

Electron spin echo detection of the microwave-induced recombination of transient radical pairs produced in photochemical reactions

Andrei V. Astashkin and Yoshio Sakaguchi

Citation: J. Chem. Phys. **106**, 9190 (1997); doi: 10.1063/1.474022
View online: http://dx.doi.org/10.1063/1.474022
View Table of Contents: http://jcp.aip.org/resource/1/JCPSA6/v106/i22
Published by the AIP Publishing LLC.

Electron spin echo detection of the microwave-induced recombination of transient radical pairs produced in photochemical reactions

Andrei V. Astashkin[a)]
The Institute of Chemical Kinetics and Combustion, 630090 Novosibirsk, Russia

Yoshio Sakaguchi[b)]
The Institute of Physical and Chemical Research (RIKEN), 351-01 Wako, Saitama, Japan

(Received 17 December 1996; accepted 4 March 1997)

The effects of the geminate recombination induced by the pulsed microwave irradiation on the electron paramagnetic resonance spectra of radicals generated in the photoinitiated hydrogen abstraction reaction of 2-methyl-1,4-naphthoquinone in a micellar sodium dodecylsulphate solution have been studied using an inversion recovery method of pulsed electron paramagnetic resonance. It was found that the stimulated nuclear polarization resulting from the microwave-induced recombination of the geminate radical pairs at one (or a limited group) of nuclear spin configurations affects the polarization and intensity of the electron paramagnetic resonance spectra of escaped radicals via the electron-nuclear cross-relaxation mechanism. The long lifetimes of the radical pairs in a micellar system facilitate the observation of the effects. Similar effects, though of much smaller scale, were found to be detectable in certain conditions also in homogeneous solutions. © *1997 American Institute of Physics.* [S0021-9606(97)01222-1]

INTRODUCTION

It is well-known that in photochemical reactions radicals are generally produced in pairs, the spin multiplicity of geminate radical pairs being determined by that of excited photochemically-active molecules.[1–3] This spin correlation of the radicals in a geminate pair lasts until it is destroyed by magnetic relaxation.[4] To stress the spin correlation of radical spins in a geminate pair, the term ''spin-correlated radical pair'' (SCRP) is also often used.

Singlet-born geminate radical pairs have a good chance to recombine immediately after their formation while triplet-born ones have to wait for the subsequent reencounters, meanwhile acquiring a singlet character due to the singlet–triplet (S–T) mixing accomplished via the so-called Δg (where g is a g factor) and hyperfine coupling mechanisms when the radicals temporarily diffuse apart.[1–3]

In weak magnetic fields the transitions between the singlet (S) and all three triplet manifolds (T_+, T_0, and T_-) are induced by a hyperfine coupling mechanism. However, if a magnetic field is strong enough ($g\beta B_0 \gg a$, where a is a hyperfine coupling constant) as it is usually the case in the X-band EPR experiments, only the $S-T_0$ mixing occurs as T_+ and T_- states are well separated from S and T_0 ones in the energy scale.

Even if the subsequent reencounters become increasingly unlikely as the time after the radical pair formation increases, the recombination channel for the triplet-born pairs provided by the $S-T_0$ mixing generally results in the underpopulation of the $S-T_0$-mixed states as compared with that of the T_+ and T_- states.

Applying a microwave (m.w.) field in resonance with EPR (electron paramagnetic resonance) transition of one of the radicals in a geminate pair, one can transfer the excessive population from the T_+ and T_- states to the mixed states and increase in this way the probability of the recombination of the triplet-born pair. For the singlet-born pair, in contrary, the population transfer from the mixed states to the empty T_+ and T_- states will decrease the recombination probability. This m.w.-induced change of reactivity of radical pairs leading to the change of the concentration of geminate recombination products and escaped radicals forms a foundation of numerous methods of reaction yield detected magnetic resonance (RYDMR).[1,5–8]

If the m.w. field affects not the whole EPR spectrum of a radical, but only one line (or a group of lines situated close to one another in the spectrum) corresponding to a given configuration of nuclear spin projections, the recombination of the radicals having this nuclear spin configuration will create a stimulated nuclear polarization (SNP) in the escaped radicals and their reaction products.[9,10]

It has been shown that the chemically-induced dynamic nuclear polarization (CIDNP) might affect the polarization of the EPR spectra via the electron-nuclear cross-relaxation mechanisms.[11,12] The effects of the cross-relaxation in the EPR spectra of radicals produced in hydrogen abstraction reactions of acetone in 2-propanol and di-*t*-butyl ketone in 2-propanol and in toluene have also been studied using a pulsed saturation recovery technique.[13,14] The saturation recovery dependences obtained were qualitatively explained based on the cross-relaxation in the escaped radicals. Though it was realized[13,14] that CIDNP should change the relative electron spin populations of the energy levels corresponding to different nuclear spin manifolds and affect the efficiency of the cross-relaxation, it proved to be difficult to clearly discern the effects of CIDNP in view of a great number of unknown parameters (the populations of various energy lev-

[a)]On leave to the Institute of Physical and Chemical Research (RIKEN), 351-01 Wako, Saitama, Japan.
[b)]Author to whom correspondence should be addressed.

 0021-9606/97/106(22)/9190/11/$10.00

els and the rates of the relaxation processes).

The saturation m.w. pulse in these studies[13,14] has been applied at long delays after the laser pulse when the concentration of the SCRP is vanishingly small and practically all radicals can be considered as the escaped ones. The saturation pulse in this condition affects only the relative populations of the electron spin energy levels, but does not change the populations in the nuclear subsystem.

In the above works,[11–14] only the EPR manifestations of a ''naturally occurring'' CIDNP were discussed. In this work, however, we have tried to detect the effect of SNP resulting from the m.w.-induced SCRP recombination on the EPR spectra of the escaped radicals. We have done the experiments with an aqueous micellar sodium dodecylsulphate solution of 2-methyl-1,4-naphthoquinone because the lifetimes of geminate radical pairs in micellar systems are fairly long. We have found that, in contrast to the usual CIDNP, the effects of the deliberately created SNP can readily be observed in the micellar system using pulsed EPR methods. Similar effects, though of much smaller scale, were found to be detectable in certain conditions also in homogeneous solutions.

EXPERIMENT

2-Methyl-1,4-naphthoquinone (methylnaphthoquinone, MNQ) was obtained from Acros and purified by recrystallization from benzene and sublimation. Sodium *n*-dodecylsulphate (SDS) was obtained from Cica–Merck. Isopropyl alcohol (99.7%, for HPLC) and *n*-dodecane were obtained from Cica–Merck and used without further purification. Distilled water (for HPLC) was obtained from Cica–Merck and purified in Iwaki UP-100 ultrapure water system by ion exchanging and ultrafine filtering. The specific resistance of the purified water used in the experiments exceeded 18 MΩ cm.

The experiments were performed with degassed solutions at room temperature, using the third harmonic (355 nm) of a Nd:YAG laser (Quanta Ray GCR-3, Spectra-Physics) as an exciting light source.

In the samples for optical measurements, the concentrations of MNQ and SDS were 0.001 and 0.08 mol dm^{-3}, respectively. In EPR experiments, the MNQ and SDS concentrations of 0.004 and 0.24 mol dm^{-3}, respectively, were typically used. We have used these high concentrations in EPR measurements in order to achieve good signal-to-noise ratios. We have checked, however, that the EPR results obtained are reproducible also at the lower concentration, same as those used for the optical studies.

The critical micellization concentration and micelle aggregation number for SDS are reported to be 0.0084 mol dm^{-3} and 60 ± 2, respectively.[15,16] It follows that both, in the optical and EPR measurements there was in the average about one MNQ molecule per micelle. As the laser pulse in our experiments has excited significantly less than 100% of MNQ molecules, the majority of micelles contained only one radical pair.

Transient EPR measurements were carried out on an

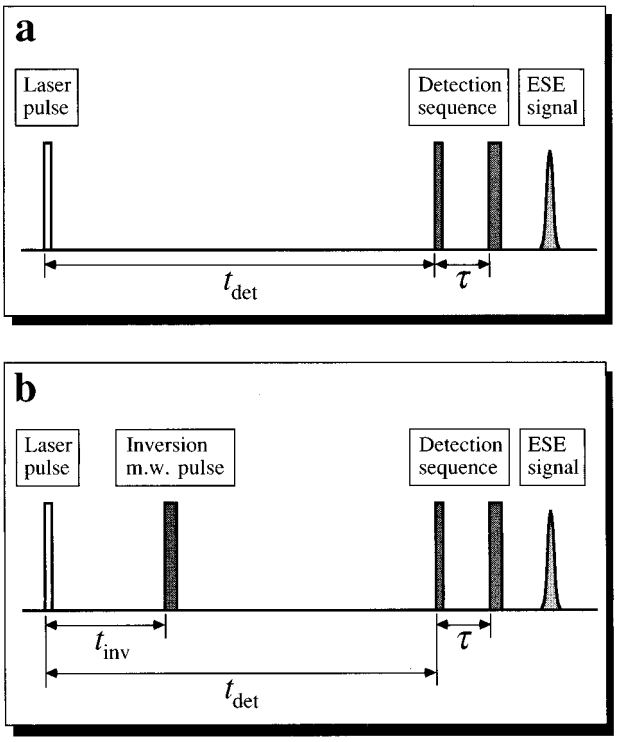

FIG. 1. The pulse sequences of the primary ESE method (a) and the inversion recovery method (b) as used in a photochemical experiment.

X-band pulsed EPR spectrometer (RSV2000, JEOL) in a continuous wave (CW) mode with a direct detection of the transient EPR signal, without magnetic-field modulation. The spectrometer was equipped with a 1 kW TWT (traveling wave tube) m.w. amplifier (Litton), rectangular TE102 cavity (unloaded $Q\approx300$) and a homemade reagent flow system.

For pulsed EPR experiments, the same spectrometer has been used. The duration of the 90° pulse was 20 ns. For the detection of transient radicals in a pulsed mode, as a rule, the two-pulse (primary) electron spin echo (ESE) method was employed [see Fig. 1(a)]. The time interval τ between the m.w. pulses was 300 ns. The ESE detection has offered an advantage that the sign of the spin polarization of the radical in various conditions could be immediately understood from the sign of the ESE signal. To suppress the free induction decay signals after the m.w. pulses, a gradient of static magnetic field (about 0.3 mT/cm) was used.

The setup for the transient optical absorption measurements was similar to that described elsewhere.[6] It consisted of two optical guides made of quartz fibre introduced into the cylindrical reagent flow cell along its axis, the exciting laser beam being normal to the cell wall. The monitoring light was supplied from the Xenon lamp through one of the optical guides. Another optical guide was connected to the monochromator and photomultiplier. The measurement wavelength was 380 nm, which is close to the optical absorption maximum of the naphthosemiquinone radical.[17]

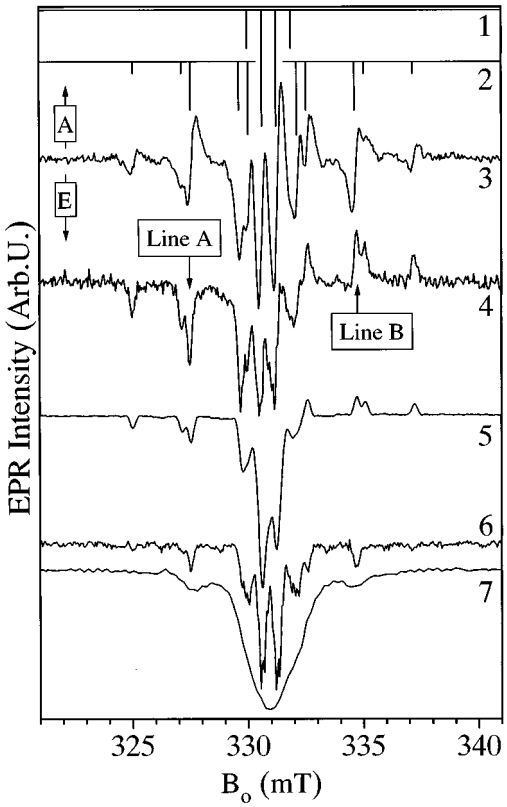

FIG. 2. Traces 1 and 2, calculated stick spectra of $MNQH^{\cdot}$ and $R^{\cdot}$, respectively, with hyperfine interaction constants given in the text. Traces 3 and 4, transient CW EPR spectra recorded with a signal integration within the delays after the laser pulse from 0 to 600 ns and from 1.2 to 3.2 μs, respectively. M.w. power, 10 mW. Trace 5, field-sweep primary ESE spectrum at $t_{det}=3\mu$s. To suppress FID, a small gradient of the static magnetic field was used. Trace 6, the field-sweep primary ESE spectrum of SCRP at $t_{det}=300$ ns obtained using a 90° out-of-phase detection. Trace 7, the EPR spectrum of SCRP measured as the m.w.-induced change of the transient optical absorption. The m.w. pulse delay, 300 ns. The m.w. pulse duration, 40 ns. The transient optical absorption signal was integrated within the delay times from 25 to 50 μs after the laser pulse. The vertical scales for all spectra are arbitrary.

RESULTS AND DISCUSSION

The illumination ($\lambda=355$ nm) of the micellar (SDS) solution of methylnaphthoquinone leads to the abstraction of a hydrogen atom by the excited triplet state of MNQ from the alkyl chain of a SDS molecule (denoted RH below) with a formation of the methylnaphthosemiquinone ($MNQH^{\cdot}$) and alkyl ($R^{\cdot}$) radicals[5,17]

$$^3MNQ^*+RH\rightarrow{}^3[MNQH^{\cdot}+R^{\cdot}]. \quad (1)$$

The EPR spectra expected for $MNQH^{\cdot}$ and $R^{\cdot}$ are shown in Fig. 2 by stick diagrams 1 and 2, respectively. The simplified spectrum of $MNQH^{\cdot}$ (trace 1, Fig. 2) was calculated using only the largest isotropic hyperfine constant of three equivalent protons of fast-rotating methyl group ($a\approx0.63$ mT).[5] To calculate the spectrum of $R^{\cdot}$ (trace 2, Fig. 2), only the large hyperfine interactions of the protons in $-CH_2-C^{\cdot}H-CH_2-$ fragment ($a\approx2.5$ mT for methylene protons and $a\approx-2.1$ mT for the proton of the radical $-C^{\cdot}H-$ group[5,18]) were taken into account. The calculated spectra are shown with the emissive polarization for the convenience of presentation.

Trace 3 in Fig. 2 shows a transient CW EPR spectrum recorded with a signal integration within the delay times after the laser pulse from 0 to 600 ns. As seen from comparison with stick diagrams 1 and 2 in the same figure, the side lines of this spectrum are contributed by $R^{\cdot}$. The center of spectrum 3 is contributed mostly by $MNQH^{\cdot}$, although the side lines of $MNQH^{\cdot}$ are overlapped with the inner lines of the spectrum of $R^{\cdot}$.

One can see that the EPR lines of $R^{\cdot}$ in spectrum 3 (Fig. 2) are split into two components, the low-field component of every line being in emission and the high field one— in absorption. This kind of ''antiphase'' line shapes was originally observed by Sakaguchi *et al.*[18] and explained independently by the groups of McLauchlan[19] and Closs[20] as arising from the $S-T_0$ mixing in a triplet-born SCRP.

When the transient EPR spectrum is recorded at longer delays after the laser pulse, the antiphase signal due to SCRP gradually decreases and, finally, disappears (trace 4 in Fig. 2). As seen from this spectrum, the low-field EPR lines of $R^{\cdot}$ are polarized emissively (E) while the high-field ones show the absorptive (A) polarization. All lines of $MNQH^{\cdot}$ are emissive, though some E/A distortion of this spectrum is also evident.

Trace 5 in Fig. 2 represents the field-sweep ESE spectrum recorded at the delay after the laser pulse $t_{det}=3\mu$s. The polarization of both radicals did not change within the delay range when the ESE signals could be observed and the field-sweep ESE spectrum was always similar to that shown by trace 5 in Fig. 2, though the relative intensity of the $MNQH^{\cdot}$ signal increased with t_{det}.

The dependeces of the absolute values of the ESE signal intensities of escaped $R^{\cdot}$ and $MNQH^{\cdot}$ on t_{det} are shown in Fig. 3(a) by open and filled circles, respectively. Under the term ''escaped radicals'' we understand the radicals that have a negligible probability of the geminate recombination and do not show the polarization characteristic of SCRP any more. In general, the intensity of the ESE signal corresponding to given EPR transition is proportional to the product of the radical concentration and the polarization of this transition. In our case, the lifetime of the escaped radicals as determined from the transient optical absorption kinetic at $\lambda=380$ nm is of the order of hundreds of microseconds (data not shown). Therefore, the dependence of the ESE signal on t_{det} reflects the dynamics of the radical polarization.

One can see from Fig. 3(a) that the buildup of the signal intensity is relatively slow, with the signal maximum being attained at the delays of 2 to 3 μs after the laser pulse. The slow decay of the ESE signals made their detection possible up to the delays of the order of 30 μs for $MNQH^{\cdot}$ and 20 μs for $R^{\cdot}$. The trace shown by open circles in Fig. 3(a) is measured for the emissive line ''A'' of the radical $R^{\cdot}$ (see Fig. 2). The dependence on t_{det} of the ESE signal corresponding to the absorptive line ''B'' of $R^{\cdot}$ (Fig. 2) was similar (data not shown).

The chemically-induced dynamic electron polarization

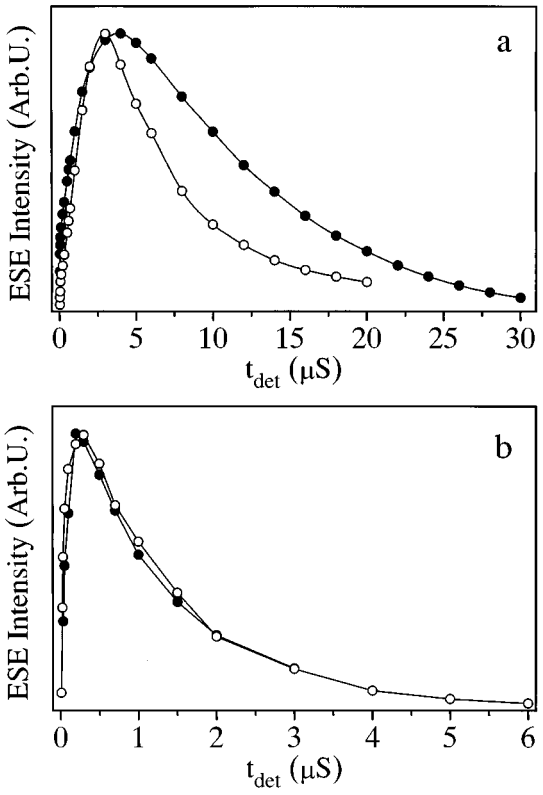

FIG. 3. (a) The dependences of the primary ESE signal intensities (sign neglected) of MNQH˙ (filled circles) and R˙ (open circles) on the delay after the laser pulse. (b) The dependence of the SCRP concentration on the delay after the laser pulse measured by the 90° out-of-phase primary ESE detection (open circles) and by the detection of the m.w.-induced change of the transient optical absorption (filled circles).

(CIDEP) mechanism creating the E/A polarization of the EPR spectrum of R˙ and the E/A distortion of the spectrum of MNQH˙ is, most probably, a so-called radical pair mechanism (RPM)[21] active in geminate pairs and in free pairs randomly formed by the escaped radicals. The net emissive polarization of MNQH˙, however, is thought to be produced by the triplet mechanism[22] because the g-factor difference for these radicals ($g \approx 2.0034$ for R˙ and $g \approx 2.0046$ for MNQH˙)[5] is too small to produce the emissive polarizations for two high-field lines of MNQH˙ via RPM. The spectrum of R˙ also shows a weak net emissive character (see traces 4 and 5 in Fig. 2), though the RPM efficiently inverts the polarization of the high-field lines to absorption. The effects of RPM are much less pronounced for MNQH˙ because its EPR signal is situated almost in the center of the considerably more broad EPR spectrum of R˙.

From this explanation it follows, for example, that the decay of the emissive ESE signal of MNQH˙ in Fig. 3(a) may be ascribed to the longitudinal relaxation of this radical. This gives for MNQH˙ an estimate of $T_1 \approx 9\,\mu$s. This relaxation time would, probably, be too long for usual nonviscous solutions, but for micellar solutions it might not be surprising.[23]

It has been experimentally and theoretically shown[24] that the SCRP with a characteristic antiphase polarization of every EPR line (as that seen for R˙ in trace 3, Fig. 2) and a time-dependent exchange interaction give a primary ESE signal with a m.w. phase shifted by 90° with respect to that observed for noninteracting radicals. We have used this result to obtain the spectrum of the SCRP in our system. Trace 6 in Fig. 2 shows a field-sweep ESE spectrum of the SCRP recorded using the 90° out-of phase ESE detection (i.e., the receiver phase was shifted by 90° with respect to that used to record the usual field-sweep ESE spectrum shown by trace 5 in the same figure). The SCRP spectrum is shown all-lines-down for the convenience of presentation only. This arrangement has no relation to the usual ''absorption-up, emission-down'' convention used for the spectra of the escaped radicals and adopted in Fig. 2.

The difference in appearance of the SCRP spectra 3 and 6 in Fig. 2 stems from the different detection methods and m.w. phases used. If the transient CW EPR spectrum were recorded in a dispersion mode (i.e., 90° out of phase, same as it was done in the ESE measurement of trace 6 in Fig. 2), the wings of the derivativelike dispersion lines corresponding to the emissively and absorptively polarized EPR transitions splitted by a small exchange interaction would add up to give a signal maximum at the spectrum position corresponding to zero exchange interaction. The CW EPR spectrum then would look qualitatively similar to that shown by trace 6 in Fig. 2. Unfortunately, this measurement option is not available with our equipment and we have to confine ourselves with these qualitative considerations that are intended to show a relation between the two spectra.

The open circles in Fig. 3(b) show the dependence of the SCRP signal intensity on the delay after the laser pulse. One can see that the maximum of the ESE signal due to the radical pairs is attained at $t_{det} \approx 250-300$ ns, with noticeable intensity being observed at the delays as long as four microseconds. This dependence qualitatively correlates with that obtained in the transient optical absorption study[17] with high time resolution.

For simplicity, we will refer to the dependences in Fig. 3(b) as those of the SCRP concentration on the delay after the laser pulse. However, one should remember, that the EPR techniques are sensitive to the population difference between energy levels that is proportional to the product of the concentration and transition polarization. For example, the ESE signal of SCRP is proportional to the population difference between $T_{\pm}$ states and $S-T_0$-mixed states. At short delays after the laser pulse, this population difference is mainly determined by the rate of the hydrogen abstraction reaction (that increases the total SCRP concentration) and by the rate of the SCRP recombination from the mixed states (that increases the population difference between them and $T_{\pm}$ states). At long delays after the laser pulse, the decrease of the SCRP ESE signal intensity is determined by the radical escape from the native micelle.

Due to the exchange interaction in SCRP, the transitions from $T_{\pm}$ to the $S-T_0$-mixed states, corresponding to the given nuclear spin configuration, have slightly different resonance fields and the EPR spectra of these pairs show the antiphase structure. Every antiphase-splitted EPR line is in

net emission or net absorption, depending on the relative contributions of the triplet CIDEP mechanism and RPM into the polarization of this line. As the intensities of the transitions from $T_{\pm}$ to the mixed states are of the same order of magnitude (even with RPM in the SCRP taken into account, but assuming the RPM polarizations induced to be much smaller than 1), the m.w. phase of the ESE signal of these pairs will be shifted close to 90° with respect to that observed for noninteracting radicals. However, some of the geminate pairs and the majority of the escaped radicals will have an exchange interaction close to zero and contribute to the ''normal'' ESE signal. It follows from this consideration that the characteristic buildup time of the ESE signals of R˙ and MNQH˙ in Fig. 3(a) (2 to 3 μs) is related to the radical escape rate.

The kinetics of the transient optical absorption of MNQH˙ were observed under the monitoring light with a wavelength of 380 nm.[17] To induce a recombination of the geminate radical pairs, a m.w. pulse of 40 ns duration was applied at the delay of 300 ns after the laser pulse. This m.w. pulse length corresponded to the inversion (180° nutation angle) of the magnetization of the escaped radicals when detected by pulsed EPR.

The choice of the nutation angle of 180° for the m.w. pulse has originated from the naive (as it did not take into account the mobility of the radicals and the resulting fast changes in the exchange coupling value) consideration that for a weak exchange interaction in a geminate radical pair the matrix element of the transition operator S_X (the axis **X** is perpendicular to the direction of the static magnetic field $\mathbf{B_0}$) is close to that realized for the escaped radicals, with the 180° pulse providing for the maximum population transfer from T_+ and T_- states to the $S-T_0$ mixed states.

Varying the external magnetic field we have found that when the m.w. pulse was in resonance with the EPR transitions of R˙ or MNQH˙, the decrease of the transient optical absorption signal of MNQH˙ occurred due to the geminate recombination stimulated by the m.w. irradiation. The EPR spectrum of the geminate radical pair detected as a change of the transient optical absorption intensity is shown by trace 7 in Fig. 2. The maximum effect was observed around the center of the MNQH˙ EPR spectrum. Even in this case, however, the decrease of the transient optical absorption signal did not exceed 10%. As the statistic weight of each of two central line groups of MNQH˙ is 3/8, one can estimate that the 10% decrease in the transient absorption signal corresponds to about 25% recombination yield of MNQH˙ affected by the m.w. pulse.

The value of the decrease of the transient absorption signal measured as a function of the m.w. pulse delay after the laser pulse is shown by filled circles in Fig. 3(b). One can see that it is similar to the dependence of the SCRP concentration obtained by the 90° out-of-phase ESE detection [open circles in Fig. 3(b)].

The optically detected spectrum 7 in Fig. 2 exhibits broad lines with a width between the maximum slope points (as estimated for resolved lines of R˙) $\Delta B_{pp} \approx 1$ mT. This width is considerably greater than the excitation width of the inversion m.w. pulse with 40 ns duration ($B_1 \sim 0.45$ mT) and we may attribute it to the exchange interactions between R˙ and MNQH˙. This conclusion is substantiated by the comparison of spectrum 7 with spectrum 5 of escaped radicals shown in the same figure. The latter spectrum is recorded with similar m.w. pulse strength but shows well-resolved line of both radicals. A numerical fitting of spectrum 7 assuming a Gaussian distribution of the exchange interaction allows one to estimate the width of this distribution to be of the order of 1 mT (data not shown). For this fitting, the exchange interaction term in a spin Hamiltonian was taken to be $2J\mathbf{S_1S_2}$, where J is an exchange interaction value.

Similar fitting of the transient CW EPR-detected spectrum 3 in Fig. 2 allows one to estimate the width of the exchange interaction distribution to be of the order of 0.25 mT. Unfortunately, it is difficult to estimate the exchange interaction for the SCRP spectrum 6 in Fig. 2 recorded using the out-of-phase ESE detection in a presence of the static magnetic-field gradient (see the Experiment section). It looks, in fact, like the spectrum of two noninteracting radicals. The reason for this effect is that the 90° out-of-phase ESE detection, due to the peculiar spin dynamics during and between the m.w. pulses,[24] is sensitive only to weak exchange interactions, $|J| < g\beta B_1$.

To explain the difference between the J values estimated from the optically detected spectrum 7 and the transient CW EPR spectrum 3 in Fig. 2, one has to take into account that radicals in a micelle are subject to Brownian motion. It is reasonable to assume that they spend most of their time spatially separated while the average duration of the reencounters is short. The exchange interaction is directly related to the distance between the radicals, with the stronger interaction corresponding to the shorter distance. Besides, greater J values correspond to greater J gradients. Thus, small changes in the interradical distance in the regions of large J will lead to large variations in the transition frequencies of the radicals of SCRP. The weak m.w. field used in transient CW EPR is unable to efficiently induce the transitions between the fast-fluctuating levels corresponding to the larger J values because the m.w. excitation width of the CW EPR method is narrow and these levels for every given radical pair are in resonance for only short time.

In contrast, the optically detected EPR spectrum 7 in Fig. 2 was measured using the pulsed excitation with high m.w. power. The m.w. excitation bandwidth was about 0.45 mT (see above). Thus, the method was relatively insensitive to the fluctuations of the transition frequencies of the same order of magnitude giving us the possibility to detect the radical pairs with stronger exchange interactions.

The above comparison shows that the values of the exchange interaction in the geminate radical pairs obtained with different methods might be significantly different. Thus, a certain caution should be exercised when comparing such data.

It is also interesting to compare the optically detected SCRP spectrum 7 in Fig. 2 with the SCRP spectrum in the same system obtained using a product yield-detected EPR

(PYEPR) method based on the spin-trapping of the escaped radicals.[5] The PYEPR spectrum[5] exhibited considerably higher resolution with the four major line groups of MNQH˙ being clearly discernible indicating a small exchange interaction of the radicals in the SCRP.

The origin of this difference is, probably, same as that of the difference in the linewidths of spectra 3 and 7 in Fig. 2 recorded using CW EPR and optical detection, respectively. Rephrasing the discussion above, we may suggest that the narrow-band excitation by weak m.w. irradiation employed in CW EPR is unable to effectively transfer the population from $T_{\pm}$ states to the mixed states (and thus enhance the probability of the SCRP recombination upon a reencounter) if the exchange interaction between radicals is excessively strong and subject to fast fluctuations.

In another work on PYEPR[8] the authors have used the pulsed m.w. irradiation of higher power (up to 4 W) to stimulate a geminate recombination of the anthrasemiquinone radical with R˙. Differentiating the dependence of the spin adduct yield on the m.w. pulse duration, they have estimated the dependence of the SCRP concentration on the delay after the laser pulse. Same as in our work, the noticeable SCRP concentration was detectable within several microseconds after the laser pulse.[8] The time profile of the SCRP concentration estimated by PYEPR,[8] though qualitatively resembling the profiles shown in Fig. 3(b) in this work, is, most probably, distorted due to the fact that the spin nutation angle (and recombination probability) for the radicals in the SCRP changes with increasing the m.w. pulse length. A strong indication that this is the case is the fact that the SCRP concentration profile[8] depended on the m.w. power used.

To observe the effects of the SCRP recombination induced by a m.w. pulse on the EPR spectra of the escaped radicals, we have used an inversion recovery pulse sequence [see Fig. 1(b)] consisting of the inversion (180°) m.w. pulse applied to the spin system after the delay t_{inv} following the laser pulse, and of the detection sequence applied after the delay t_{det}. The detection sequence consisted of two m.w. pulses separated by the time interval τ (typically, 300 ns), forming a primary ESE signal.

This pulse train is essentially similar to the saturation recovery sequence employed elsewhere[13,14] to elucidate the manifestations of the electron–nuclear cross relaxation in the EPR spectra of escaped radicals. In those works, however, the effects of the m.w.-induced recombination of the geminate radical pairs have not been studied. The difference between the inversion and saturation recovery sequences consists in the choice of the nutation angle of the first m.w. pulse, 180° (the inversion pulse) in this work instead of 90° (saturation pulse) used by the authors of Refs. 13 and 14.

The inversion recovery measurements were performed in two different ways. In the first modification t_{inv} was fixed and t_{det} was varied. The ESE signal intensity was measured as a function of t_{det}. In the second modification the ESE signal intensity was measured as a function of t_{inv} while t_{det} was maintained constant.

Figure 4(a) shows the inversion recovery dependences

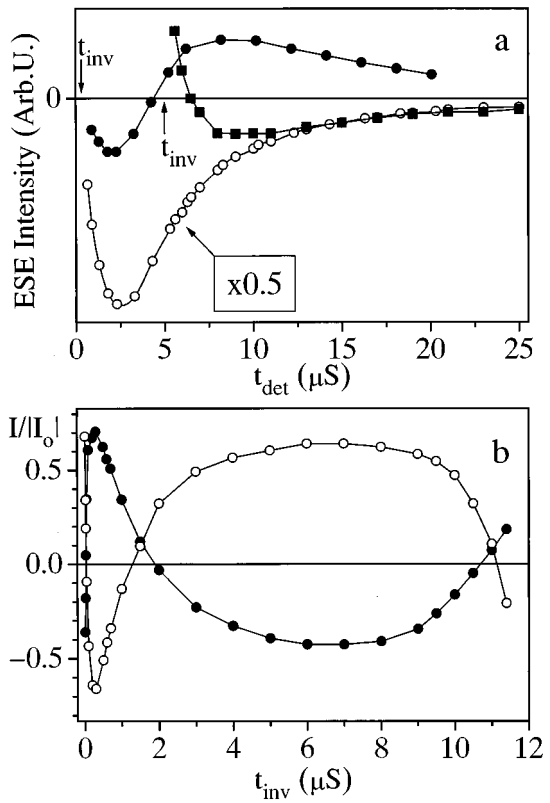

FIG. 4. (a) Open circles, the dependence of the primary ESE signal of the emissive line ''*A*'' (see Fig. 1) of R˙ on the delay after the laser pulse. Filled circles, the inversion recovery dependence for $t_{\mathrm{inv}}=300$ ns and t_{det} varied (same EPR line). Filled squares, the inversion recovery dependence for $t_{\mathrm{inv}}=5$ μs and t_{det}varied (same EPR line). The arrows marked ''t_{inv}''show the positions of the inversion pulse for both traces. (b) Filled and open circles, the inversion recovery dependences for the emissive (''*A*'', see Fig. 1) and absorptive (''*B*'') lines of R˙, respectively, obtained with $t_{\mathrm{det}}=12$ μs and t_{inv} varied. The signal intensities are normalized by the intensity obtained without the inversion pulse.

obtained for the emissive line ''*A*'' in the R˙ spectrum shown in Fig. 2. In this experiment, the position of the inversion pulse t_{inv} was fixed and that of the detection sequence t_{det} was varied. Depending on t_{inv}, two qualitatively different types of dependences were obtained.

If the inversion pulse was applied at t_{inv} exceeding the time range of the existence of considerable concentration of the SCRP [see Fig. 3(b)], a clear inversion of the ESE signal of R˙ was observed at short $\Delta t_d = t_{\mathrm{det}} - t_{\mathrm{inv}}$, followed by its fast decrease and change of sign as Δt_d increased. The sense of the signal polarization then remained same as it was without inversion until large Δt_d values, when the signal was practically lost in noise. An example of this kind of a dependence is given by the trace measured for $t_{\mathrm{inv}}=5$ μs and shown in Fig. 4(a) by solid squares. The trace shown in the same figure by open circles is a dependence of the R˙ (line *A*) ESE signal intensity on the delay after the laser pulse (without the inversion pulse) and is given for comparison. This dependence is essentially similar to that shown by open circles in Fig. 3(a), however, with the sign of the ESE signal polarization being retained.

If the inversion pulse was applied at short t_{inv}, when the concentration of the SCRP was close to maximum, the inversion recovery dependence was noticeably different as exemplified by the trace measured for $t_{inv}=300$ ns (close to the maximum of the SCRP concentration) shown in Fig. 4(a) by solid circles. Now the inverted signal amplitude rapidly decreased with increasing Δt_d and changed sign to opposite. As a result, at $\Delta t_d=600$ ns (it was minimum Δt_d that allowed the observation of the pure primary ESE signal formed by the detection sequence, without overlap with the unwanted echoes) the sense of the polarization was already same as that without the inversion pulse. With further increase of Δt_d, the signal intensity first increased, the sense of the polarization being same as that without the inversion pulse. After reaching a maximum at $t_{det}\approx 2$ μs, the signal decreased and changed the sign of the polarization at $t_{det}\approx 4$ μs. The polarization then remained opposite to the original one until large Δt_d.

Similar dependences were obtained for the absorptive line ''*B*'' in the spectrum of R˙ presented in Fig. 2 (data not shown). The polarizations of the ESE signals in this case were opposite to those presented in Fig. 4(a).

To understand the inversion recovery dependences obtained, we have to consider qualitatively the mechanisms governing the populations of the energy levels in our radical system. We will use as a model a simplified diagram in which only the electron spin populations in three nuclear spin manifolds corresponding to the total nuclear spin projections Σm_I equal to $M-1$, M, and $M+1$ are shown, the levels with $\Sigma m_I=M$ being those affected by the m.w. pulses (see Fig. 5). To model the situation for the emissive line *A* in the spectrum of R˙, the populations of the upper levels in the escaped radicals corresponding to $m_S=+1/2$ are taken to be greater than those of the lower levels ($m_S=-1/2$). This population distribution is shown in Fig. 5(b). For simplicity, the populations of the levels with similar electron spin projections are taken to be similar, though it is not the case in a real system, especially with degenerate energy levels corresponding to several nuclear spin configurations. This assumption suits the purposes of our qualitative consideration and is never used explicitly. However, in any quantitative treatment it should be removed. The assignment to the total nuclear spin projections is given in the bottom of every panel in the figure.

Consider first the situation of long t_{inv} represented by the trace shown by solid squares in Fig. 4(a). Immediately after the inversion pulse the populations of the energy levels $|\alpha,M\rangle$ and $|\beta,M\rangle$ of the escaped radicals are inverted [see Fig. 5(c)] giving an absorptive ESE signal. If only the longitudinal relaxation were active in the system, this signal had to remain absorptive with an amplitude approaching the Boltzmann equilibrium value as t_{det} increased. From Fig. 4(a) one can see, however, that the signal changes sign and then remains emissive until long t_{det}. Therefore, we have to consider other processes governing the populations of the energy levels.

One mechanism to take into account is a cross relaxation with simultaneous change of the electron and nuclear spin projections. In a radical fragment of R˙, $-CH_2-C^{\cdot}H-CH_2-$, most of the protons responsible for the large hyperfine splittings are in the β position with respect to the radical carbon atom. As the anisotropic hyperfine interaction for the β protons is small compared with the isotropic one,[25] the prevailing cross-relaxation mechanism for R˙ is expected to be the scalar one, with a selection rule $\Delta m_S+\Delta m_I=0$. This cross relaxation in R˙ will be induced by the conformational changes in the aliphatic chain. The scalar cross-relaxation transitions are shown in Fig. 5 by diagonal arrows in the energy level diagrams of the escaped radicals.

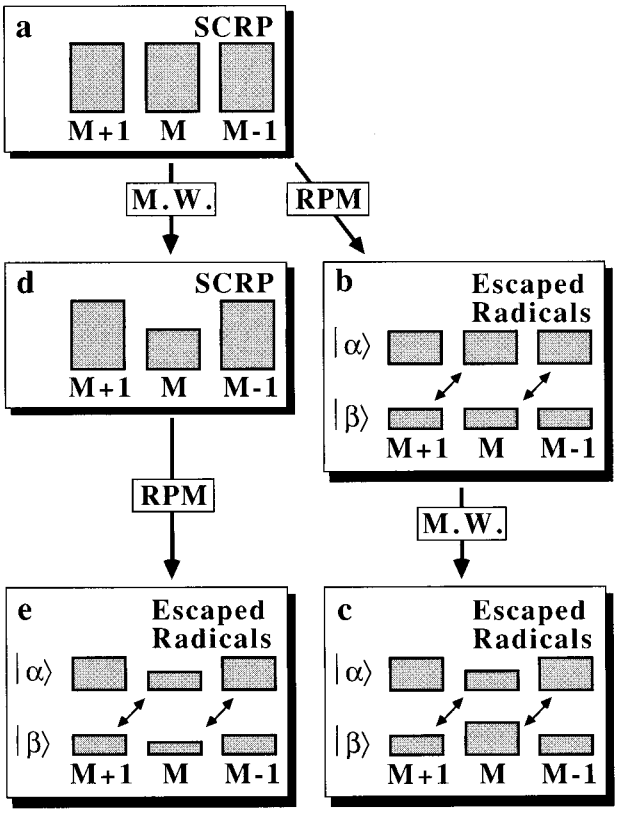

FIG. 5. The diagram showing qualitatively the effect of the 180° m.w. pulse on the populations in various electron and nuclear spin manifolds of SCRP (a and d) and escaped radicals (b, c, and e). The total nuclear spin projections for various electron spin energy levels are given in the bottom of every panel. The electron spin transition corresponding to the total nuclear spin projection *M* is in resonance with the m.w. field. Diagonal arrows in the energy level diagrams of escaped radicals (b, c, and e) show the scalar cross-relaxation transitions. See the text for the detailed explanation.

We will not consider here the cross-relaxation transitions with the selection rule $\Delta m_S+\Delta m_I=2$ caused by the anisotropic hyperfine interactions modulated by the molecular reorientations. In a radical fragment of R˙ there is only one α proton with strong anisotropic hyperfine interaction[25] and the statistic weight of the cross-relaxation transitions with $\Delta m_S+\Delta m_I=2$ is considerably smaller than that of the scalar transitions. Also in MNQH˙ that will be briefly discussed below, the β protons of the fast-rotating CH_3 group have the isotropic hyperfine couplings of about 0.63 mT, far exceeding all other hyperfine interactions in the radical and ensur-

ing the predominance of the scalar cross-relaxation mechanism.

Yet another process to be considered is the CIDEP mechanism creating the emissive polarization of the low-field lines of $R^{\cdot}$ and the absorptive polarization of the high-field ones. As mentioned above, it might be RPM active in geminate and random radical pairs.

The populations of the upper energy levels in Fig. 5(b) are greater than those of the lower ones. Therefore, the longitudinal and cross relaxation will tend to restore the absorptive polarization thus competing with RPM that maintains the emissive polarization. As the polarization of the low-field lines of $R^{\cdot}$ remains emissive until long delay times after the laser pulse, we can conclude that the polarization process by RPM is more efficient than the relaxational depolarization.

After the populations in the levels with $\Sigma m_I = M$ are inverted [Fig. 5(c)], the efficiency of the cross relaxation decreases because the corresponding population differences decrease. This imbalance between all the processes works in favor of RPM which will tend to restore to some extent the emissive polarization of the transition between the levels with $\Sigma m_I = M$ as it is observed in the experimental inversion recovery dependence obtained at long t_{inv}. We believe this is a main mechanism responsible for the change of the inverted ESE signal back to emission.

Another situation occurs when the inversion m.w. pulse is applied at short t_{inv}, when there exists a large concentration of SCRP. In this case a considerable part of the radical pairs are characterized by a weak (of the order of several mT) exchange interaction. For every nuclear spin configuration, the four electron spin functions of the two-radical system can be written in the basis of triplet ($T_+ = |\alpha\alpha\rangle$, $T_0 = (|\alpha\beta\rangle + |\beta\alpha\rangle)/2^{1/2}$, $T_- = |\beta\beta\rangle$) and singlet ($S = (|\alpha\beta\rangle - |\beta\alpha\rangle)/2^{1/2}$) wave functions as T_+, T_-, $cT_0 + sS$, and $-sT_0 + cS$ with the factors c and s being determined by the relative values of hyperfine, electron Zeeman and exchange interactions. The exchange interaction is assumed to be small compared to the Zeeman one to provide for only the S–T_0 mixing to be efficient. It is shown that for the triplet-born radical pair with the initial populations of all triplet states being close to 1/3, the population of the mixed states will be smaller than that of the T_+ and T_- ones.[19,20] This population distribution is manifested in the EPR spectra of radical pairs as the characteristic antiphase appearance of the resonance lines (see Refs. 19, 20, and trace 3 in Fig. 2).

The inversion m.w. pulse will transfer the large population from the T_+ and T_- states of the SCRP with $\Sigma m_I = M$ to the mixed states.[26] This population transfer will increase the recombination probability of the radical pairs with $\Sigma m_I = M$ in subsequent reencounters. As a result, the number of radical pairs with this nuclear spin configuration will decrease compared to that observed without the m.w. pulse. The initial (before m.w. irradiation) and final (after the m.w.-induced recombination) states of the SCRP are given in Figs. 5(a) and 5(d), respectively, without details of the electron spin energy level structure. The area of the filled rectangles in Figs. 5(a) and 5(d) shows qualitatively the total populations in different nuclear spin manifolds, irrespective of their distribution over the electron spin projections. The result of the m.w.-induced recombination is seen in Fig. 5(d) as the decrease of the total number of the radical pairs with $\Sigma m_I = M$.

As the recombination of the radicals in our model is selectively enhanced for one (or a limited group) of the nuclear spin configurations only, the SNP will be created in the escaped radicals as a result of this reaction. The manifestations of the nonequilibrium nuclear polarization in changing the electron spin polarization across the EPR spectrum have been already discussed.[11,12] Here we will apply the general ideas described in Refs. 11 and 12 to our situation.

Assuming the nuclear spin projections to be conserved in the processes of the CIDEP formation for the escaped radicals, one can picture the populations of the energy levels of the escaped radicals as those presented in Fig. 5(e), with the populations of the levels with $\Sigma m_I = M$ being reduced as compared with those shown in Fig. 5(b).

One has to take into account that not all the pairs affected by the m.w. pulse will reencounter and recombine. At short t_{inv} some SCRPs have the exchange interaction strong enough to shift the frequency of the $|\alpha,M\rangle \leftrightarrow |\beta,M\rangle$ transition out of resonance with the inversion m.w. pulse. These radicals, therefore, will not be affected by the m.w. pulse significantly. With increasing Δt_d the radicals in these pairs will diffuse apart, the exchange interaction between them will decrease and the transition frequencies of the radicals will become similar to those in the escaped radicals.

All the radicals that survive after the inversion m.w. pulse will take part in a normal process of the CIDEP formation (via, e.g., RPM mechanism) and contribute to the emissive population distribution in the energy levels corresponding to the low-field lines of the escaped radicals $R^{\cdot}$. This process is thought to be responsible for the increase of the emissive ESE signal at short Δt_d in the trace obtained at $t_{\mathrm{inv}} = 300$ ns and shown by filled circles in Fig. 4(a). It, however, does not change the qualitative appearance of population distribution shown in Fig. 5(e).

At long Δt_d the cross relaxation will transfer the excessive population from the levels $|\alpha,M-1\rangle$ and $|\beta,M+1\rangle$ to the levels $|\beta,M\rangle$ and $|\alpha,M\rangle$, respectively, and contribute to the absorptive (as the population of the level $|\alpha,M-1\rangle$ is greater than that of $|\beta,M+1\rangle$) character of the ESE signal. The population differences between the levels coupled by the cross-relaxation transitions in Fig. 5(e) are considerably greater than those in Figs. 5(b) and 5(c). Therefore, one may expect that the absorptive contribution due to cross relaxation can overcome the emissive contribution of RPM in the $\Sigma m_I = M$ nuclear spin manifold as it happens in the experimental inversion recovery trace shown by filled circles in Fig. 4(a).

From the above considerations one can see that the polarization of a given EPR transition detected at given t_{det} depends on the SCRP concentration present at t_{inv}. It is interesting, therefore, to measure directly the polarization at fixed t_{det} as a function of t_{inv}. This kind of a dependence measured for the lines of $R^{\cdot}$ marked A and B in Fig. 2 is shown in Fig. 4(b) by solid and filled circles, respectively. In

this experiment, t_{det} was equal to 12 μs and t_{inv} was varied from 10 ns to 11.4 μs. One can see that at small Δt_d (i.e., t_{inv} only slightly smaller than t_{det}) the sign of the ESE signal is opposite to that observed without the inversion pulse. As t_{inv} decreases, the ESE signal amplitude approaches zero and changes its sign to opposite.

This behavior is qualitatively similar to that shown by the trace drawn in solid squares in Fig. 4(a) and was discussed above. To see the relation between the two traces more clearly, one has to take into account that in Fig. 4(b) Δt_d increases with *decreasing* the abscissa argument (t_{inv}) and in Fig. 4(a) Δt_d increases with *increasing* the argument (t_{det}). Therefore, the region of the inversion recovery dependences in Fig. 4(b) at small enough Δt_d ($\Delta t_d \leqslant 8\,\mu$s, $t_{inv} \geqslant 4$ μs) is just a reflected in a horizontal direction replica of the trace shown by solid squares in Fig. 4(a).

At still shorter t_{inv} the inversion pulse affects relative spin orientation in the SCRP. The recombination of part of the radical pairs leads to the imbalance in the electron spin population distribution in the escaped radicals. This increases the efficiency of the cross relaxation which eventually creates the polarization opposite to the original one as explained above. The effect peaks at $t_{inv} \approx 200-300$ ns, which correlates well with the time delay when the maximum concentration of the SCRP is observed [see Fig. 3(b)]. The profiles of the indentations at short t_{inv} in the inversion recovery dependences shown in Fig. 4(b) are similar to the profile of the SCRP concentration presented in Fig. 3(b).

The field-sweep ESE spectra at $t_{det}=12\mu$s obtained using a two-pulse sequence [Fig. 1(a)] and the inversion recovery sequence [Fig. 1(b)] with $t_{inv}=300$ ns are shown by traces 1 and 2 in Fig. 6, respectively. The sign inversion of the spectrum of $R^{\cdot}$ is clearly visible. The m.w. effect on the spectrum of $MNQH^{\cdot}$ at this particular settings of t_{det} and t_{inv} is considerably less pronounced, probably, because of the difference in the cross-relaxation efficiencies in $R^{\cdot}$ and $MNQH^{\cdot}$.

Figure 7(a) shows the inversion recovery dependences of similar kind (t_{det} fixed, t_{inv} varied) obtained for the low- and high-field groups of lines of $MNQH^{\cdot}$ (filled and open circles, respectively) corresponding to maximum and minimum total spin projections of 2-methyl protons, respectively. One can see that at $t_{inv} \approx 300$ ns the polarization of the low-field line of $MNQH^{\cdot}$ has changed to opposite. The polarization of the high-field line has remained same, but the signal amplitude has increased about three times. The effect for two inner lines (not shown) was intermediate between these two limiting cases. Same as we have seen for $R^{\cdot}$, the overall effect qualitatively looked as the addition of the A/E polarization pattern to the initial signal.

The inversion recovery dependences for $MNQH^{\cdot}$ can also be rationalized with the qualitative model considered above. For the side lines of $MNQH^{\cdot}$ only one cross-relaxation transition in Fig. 5(e) should be considered, $|\alpha,M-1\rangle \leftrightarrow |\beta,M\rangle$ or $|\alpha,M\rangle \leftrightarrow |\beta,M+1\rangle$, resulting whether in absorptive or emissive contribution to the polarization.

It is interesting to note that the observed relative changes

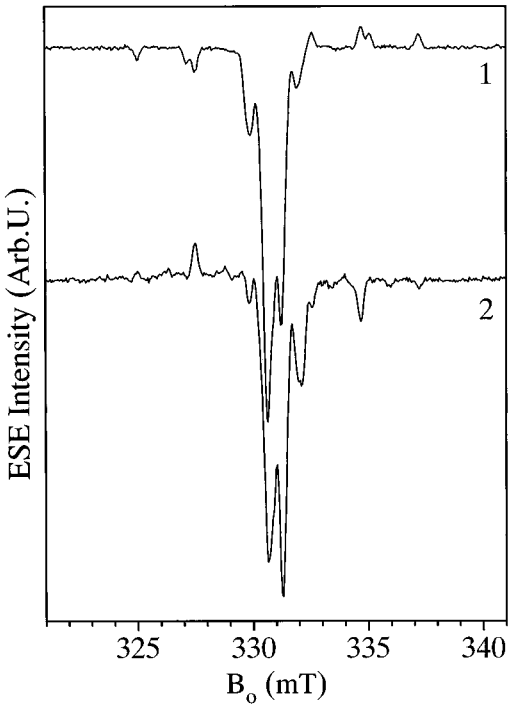

FIG. 6. Traces 1 and 2, the field-sweep ESE spectra at $t_{det}=12$ μs obtained using a two-pulse sequence and the inversion recovery sequence with $t_{inv}=300$ ns, respectively.

of the intensities of the EPR lines induced by the SCRP recombination are greater than 100%. This situation contrasts with the detection of the SCRP recombination using the optical absorption measurements. In the latter case the effect is equal to the fraction of the radicals that recombine under the action of the m.w. pulse and cannot be greater than 100% (in fact, for the central line groups of $MNQH^{\cdot}$ the effect was about 10%). The reason for the large EPR effects is that the EPR detection is selective with respect to the nuclear spin configuration of the radicals. Besides, the population transfer from other energy levels can create a population difference in a nuclear spin manifold with $\Sigma m_I = M$ greater than the original one even if the total population of these levels may remain small. This means that, in favorable conditions the electron spin echo detection might be relatively much more sensitive than the optical detection of the SCRP recombination.

It was interesting to try to detect the effects of the radical pair recombination induced by the m.w. irradiation also in homogeneous solutions. In this case, the lifetime of the geminate radical pair at room temperature is usually very short, of the order of 10^{-9} s, and there is not enough time to reorient noticeably the spin of one of the radicals in the pair using a m.w. field with $B_1 \leqslant 1$ mT typically available in our experiments. Therefore, the effects, if observable, were expected to be extremely small. Indeed, we have failed to observe any effects due to the SCRP recombination for MNQ dissolved in *n*-dodecane (data not shown) where the hydrogen abstraction reaction similar to that described by Eq. (1) takes place.

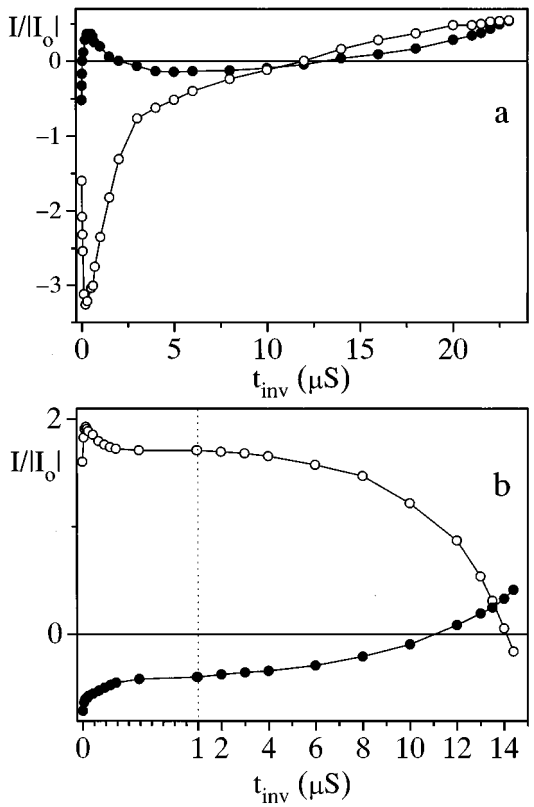

FIG. 7. (a) Filled and open circles, the inversion recovery dependences for the low- and high-field side lines of $MNQH^{\cdot}$,respectively, obtained with $t_{det}=24$ μs and t_{inv} varied. Sample, $MNQ/SDS/H_2O$. (b) Filled and open circles, the inversion recovery dependences for the low- and high-field side lines of $MNQH^{\cdot}$, respectively, obtained with $t_{det}=15$ μs and t_{inv} varied. Sample, MNQ/2-propanol. The horizontal scale between $t_{inv}=0$ and 1 μs (to the left from the vertical dashed line) is expanded but linear. The signal intensities are normalized by the intensity obtained without the inversion pulse.

However, for MNQ dissolved in 2-propanol (the hydrogen abstraction by MNQ from 2-propanol) the SCRP recombination effects in the inversion recovery dependences were observable. This is exemplified by Fig. 7(b) where the inversion recovery traces for the low- and high-field line groups of $MNQH^{\cdot}$ are shown. In this case the polarization pattern of the $MNQH^{\cdot}$ spectrum at large delays after the laser pulse was different from that observed for MNQ in SDS, with low-field peaks of the spectrum being in emission and high-field peaks—in absorption. The reason for this change of the polarization compared to the micellar system represents a subject of a separate study and falls out of the scope of this paper. The effect due to the SCRP recombination is evident as an indention in the inversion recovery traces at short t_{inv} ($t_{inv} \leqslant 300$ ns). This experiment shows that it is possible to detect the effects due to the m.w.-induced recombination of the radical pairs by pulsed EPR even in a homogeneous solution if its viscosity is not too low.

In this work we have shown that the stimulated nuclear polarization resulting from the microwave-induced recombination of the geminate radical pairs at one (or a limited group) of nuclear spin configurations can seriously affect the polarization and intensity of the EPR spectra of the escaped radicals via the electron-nuclear cross-relaxation mechanism. The long lifetimes of the radical pairs in micellar systems facilitate the observation of the effects. It is shown, however, that they can be observed also in some homogeneous solutions provided their viscosity is not too low and the cross relaxation in the radicals is faster or comparable to the rate of the polarization decay. It is also shown that the relative change of the intensity of the EPR transition affected by the m.w. inversion pulse can be much greater than the change of the transient optical absorption. This effect is thought to facilitate the observation of the radical pair recombination by the inversion recovery method in homogeneous solutions.

Finally, we have to note that in the part related to the observation of the cross-relaxation effects in ESE this work was technically similar to the other ESE studies.[13,14] Though the motivation of those works was different (see Introduction), the discussion of the cross-relaxation effects in ESE given there was extremely helpful in interpreting the effects of the SCRP recombination observed in this work using an ESE inversion recovery method.

ACKNOWLEDGMENTS

Y.S. acknowledges support by Grant-in-Aid for Scientific Research (07804037) from the Ministry of Education, Science, and Culture of Japan and by the MR Science Research Project of RIKEN. A.V.A. is grateful to RIKEN for awarding him a collaborative scientist position in the Molecular Photochemistry Laboratory. Last but not least, the authors are greatly indebted to Dr. Hisaharu Hayashi, Head of the Molecular Photochemistry Laboratory, RIKEN, for his helpful and stimulating discussion and for his continuing encouragement.

[1] K. M. Salikhov, Yu. N. Molin, R. Z. Sagdeev, and A. L. Buchachenko, *Spin Polarization and Magnetic Effects in Radical Reactions* (Elsevier, Amsterdam, 1984).
[2] H. Hayashi, in *Photochemistry and Photophysics*, edited by J. F. Rabek (CRC, Boca Raton, Florida, 1990), Vol. I, p. 59.
[3] H. Hayashi and Y. Sakaguchi, in *Lasers in Polymer Science and Technology: Applications*, edited by J.-P. Fouassier and J. F. Rabeck (CRC, Boca Raton, Florida, 1990), Vol. II, p. 1.
[4] H. Hayashi and S. Nagakura, Bull. Chem. Soc. Jpn. **57**, 322 (1984).
[5] M. Okazaki, S. Sakata, R. Konaka, and T. Shiga, J. Chem. Phys. **86**, 6792 (1987).
[6] A. I. Grant, K. A. McLauchlan, and S. R. Nattrass, Mol. Phys. **55**, 557 (1985).
[7] S. N. Batchelor, K. A. McLauchlan, and I. A. Shkrob, Chem. Phys. Lett. **181**, 327 (1991).
[8] M. Okazaki, K. Toriyama, Yu. Tai, and T. Shiga, in *Spin Chemistry*, edited by Y. J. I'Haya (The Oji International Conference on Spin Chemistry, Tokyo, 1991), p. 258.
[9] E. G. Bagryanskaya, Yu. A. Grishin, R. Z. Sagdeev, and Yu. N. Molin, Chem. Phys. Lett. **114**, 138 (1985).
[10] N. I. Avdievich, E. G. Bagryanskaya, Yu. A. Grishin, and R. Z. Sagdeev, Chem. Phys. Lett. **155**, 141 (1989).
[11] V. I. Valyayev, Yu. N. Molin, R. Z. Sagdeev, P. J. Hore, K. A. McLauchlan, and N. J. K. Simpson, Mol. Phys. **63**, 891 (1988).
[12] F. Jent and H. Paul, Chem. Phys. Lett. **160**, 632 (1989).
[13] P. P. Borbat, A. D. Milov, and Yu. N. Molin, Chem. Phys. Lett. **164**, 330 (1989).
[14] P. P. Borbat, A. D. Milov, and Yu. N. Molin, in *Spin Chemistry*, edited by Y. J. I'Haya (The Oji International Conference on Spin Chemistry, Tokyo, 1991), p. 353.

[15] P. Mukerjee and K. J. Mysels, Natl. Stand. Ref. Data Ser., Natl. Bur. Stand. No. 36 (1971).
[16] N. J. Turro and A. Yekta, J. Am. Chem. Soc. **100**, 5951 (1978).
[17] Y. Sakaguchi and H. Hayashi, J. Phys. Chem. **88**, 1437 (1984).
[18] Y. Sakaguchi, H. Hayashi, H. Murai, and Y. J. I'Haya, Chem. Phys. Lett. **110**, 275 (1984).
[19] C. D. Buckley, D. A. Hunter, P. J. Hore, and K. A. McLauchlan, Chem. Phys. Lett. **135**, 307 (1987).
[20] G. L. Closs, M. D. E. Forbes, and J. R. Norris, Jr., J. Phys. Chem. **91**, 3592 (1987).
[21] F. J. Adrian, J. Chem. Phys. **54**, 3918 (1971).
[22] S. K. Wong, D. A. Hutchinson, and J. K. S. Wan, J. Chem. Phys. **58**, 985 (1973).
[23] N. E. Polyakov, M. Okazaki, Y. Konishi, and K. Toriyama, J. Phys. Chem. **99**, 15108 (1995).
[24] M. C. Thurnauer and J. R. Norris, Chem. Phys. Lett. **76**, 557 (1980).
[25] A. Carrington and A. D. McLachlan, *Introduction to Magnetic Resonance* (Harper & Row, New York, 1969).
[26] In case of SCRP, the nuclear spin projections m_I refer to only one radical of the pair, the one that is affected by the m.w. pulse and is shown in the diagrams of escaped radicals [Figs. 5(b), 5(c), and 5(e)]. The nuclear spin projections of the other radical are arbitrary.